EPJ Web of Conferences **364**, 04012 (2026) https://doi.org/10.1051/epjconf/202636404012
Quark Matter 2025

Unveiling the dynamics of long-range correlations in high-multiplicity jets through substructure engineering in pp collisions at CMS

Xiaoyu Liu[1,*] for the CMS Collaboration

[1]Rice University, 6100 Main St, Houston, TX 77005, USA

Abstract. Recent CMS data have revealed long-range correlations at high charged-particle multiplicity ($N_{\mathrm{ch}}^{\mathrm{j}}$) within jets produced in proton-proton (pp) collisions, suggesting collective behavior in systems much smaller than those typical of heavy ion collisions. In the polar coordinate system about the reconstructed jet axis, two-particle azimuthal correlations show an unexpected rise in elliptic anisotropy (v_2^*) at large pseudorapidity separations ($\Delta\eta^* > 2$) as a function of $N_{\mathrm{ch}}^{\mathrm{j}}$, a trend not reproduced by event generators like PYTHIA or SHERPA. In this paper, we present detailed measurements of long-range correlations using LHC Run 2 data for pp collisions at $\sqrt{s} = 13$ TeV and compare the results with model predictions. The transverse momentum and $\Delta\eta^*$ dependence of v_2^* is shown across a wide range in $N_{\mathrm{ch}}^{\mathrm{j}}$. Furthermore, the role of jet substructure, particularly in jets exhibiting two-prong features, is examined to unveil a potential connection between the v_2^* enhancement and the initial-state jet geometry. A surprising increase in v_2^* emerges exclusively in these two-prong jets at high $N_{\mathrm{ch}}^{\mathrm{j}}$.

1 Introduction

Collective behavior, long established in heavy-ion collisions, has also been observed in smaller systems such as proton-proton (pp), proton-nucleus (pA), and lighter AA systems, where large final-state multiplicities indicate high initial parton densities, raising the possibility of forming tiny QGP droplets [1]. More recently, it has been suggested that collectivity could even emerge from the fragmentation and hadronization of a single energetic parton in the QCD vacuum [2]. To test this, high-multiplicity jets in pp collisions were proposed as a laboratory, defining particle kinematics relative to the jet axis ("jet frame"). The CMS collaboration [3] has reported the first evidence of long-range azimuthal anisotropy inside such jets at $\sqrt{s} = 13$ TeV. This enhancement is absent in conventional fragmentation models like PYTHIA8 and SHERPA, but can be reproduced by including parton shower rescattering [4], reminiscent of hadronic collision dynamics confined within the jet frame. In this work, we extend the CMS study with new differential measurements. A key novelty is the selection of jets with pronounced two-prong substructure to examine their role in generating collectivity. These results provide new insights into the interplay between the jet substructure and final-state interactions.

*e-mail: xl155@rice.edu

2 Experimental setup

The $\sqrt{s}$ = 13 TeV pp collisions used in this analysis were delivered from 2016–2018 and correspond to an integrated luminosity of 138 fb^{-1}. The data were collected using an online trigger searching for events containing anti-jets [5] with distance parameter R = 0.8 having a transverse momentum ($p_{\mathrm{T}}^{\mathrm{jet}}$) above 500 GeV. In the offline analysis, jets were required to have $p_{\mathrm{T}}^{\mathrm{jet}} > 550$ GeV and pseudorapidity $\left|\eta^{\mathrm{jet}}\right| < 1.6$ in the laboratory reference frame.

This analysis is particularly interested in the charged particles of jets. These charged particles are required to have $|\eta| < 2.4$ and $p_{\mathrm{T}} > 0.3$ GeV in the laboratory reference frame. Additionally, they must have a p_{T} uncertainty of $< 10\%$, and a distance of closest approach significance with respect to the primary vertex of at most three standard deviations (σ) [6]. The PUPPI algorithm [7, 8] is used to mitigate the effect of pileup at the reconstructed particle level, using local shape information, event pileup properties, and tracking information. Jets are classified into different classes based on the number of charged particles of the jet passing these selections and PUPPI subtraction before correcting for detector effects.

3 Results

3.1 The $\Delta\eta^*$ and j_{T} dependence of two-particle correlations

The focus of this analysis is to further explore the dependence of the extracted long-range azimuthal anisotropies on the minimum pseudorapidity separation ($\Delta\eta^*_{\mathrm{min}}$). The prominence of long-range correlations is enhanced by increasing $\Delta\eta^*_{\mathrm{min}}$, as this suppresses short-range correlations. Figure 1 presents v_2^* as a function of $\Delta\eta^*_{\mathrm{min}}$ for $0.3 < j_{\mathrm{T}} < 3$ GeV (j_{T} being p_{T} in the jet frame), across eight $N_{\mathrm{ch}}^{\mathrm{j}}$ intervals. This behavior aligns with the predictions of a model incorporating final-state partonic rescattering in the parton shower [4], further supporting the possibility of emergent collective behavior in high-multiplicity jets.

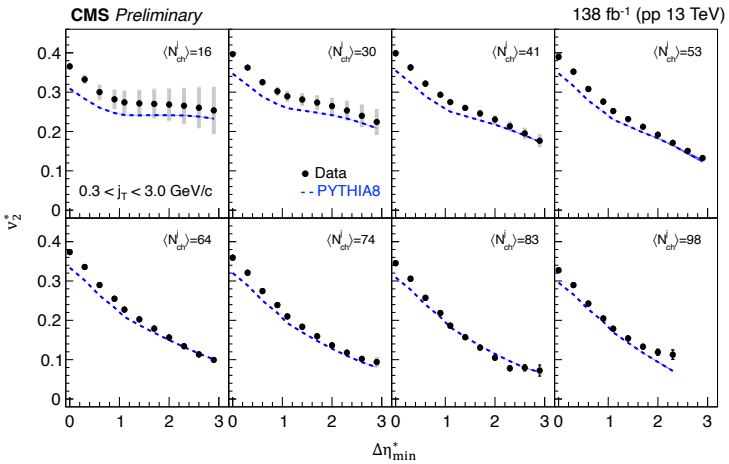

Figure 1. The elliptic anisotropy coefficient v_2^*, obtained from two-particle correlations, as a function of the minimum $\Delta\eta^*$ limit for eight $N_{\mathrm{ch}}^{\mathrm{j}}$ intervals. Results correspond to anti- R = 0.8 jets with $p_{\mathrm{T}}^{\mathrm{jet}} > 550$ GeV and $\left|\eta^{\mathrm{jet}}\right| < 1.6$ in collisions at 13 TeV. Data points include statistical uncertainties (vertical bars), while systematic uncertainties are represented by shaded boxes. The shaded envelope around the PYTHIA8 model curves indicates statistical uncertainty.

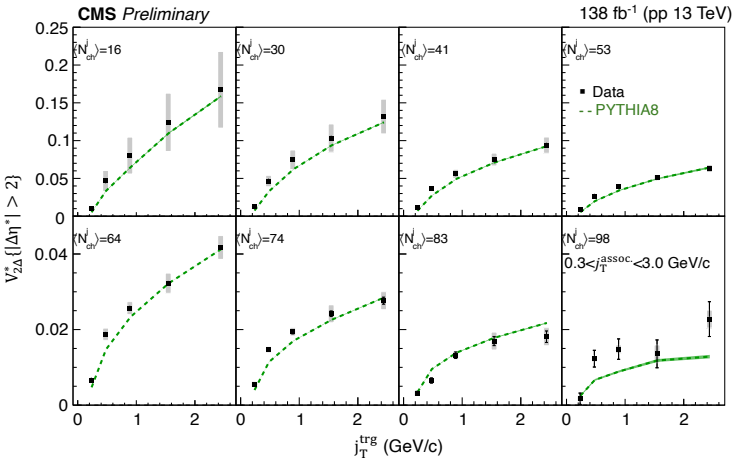

Figure 2. The second-order two-particle Fourier coefficient, $V^*_{2\Delta}$, as a function of $j_{\mathrm{T}}^{\mathrm{trg}}$ for different $N_{\mathrm{ch}}^{\mathrm{j}}$ ranges, with associated particles in the range $0.3 < j_{\mathrm{T}}^{\mathrm{ass}} < 3\,\mathrm{GeV}$. Results are shown for anti- R = 0.8 jets with $p_{\mathrm{T}}^{\mathrm{jet}} > 550\,\mathrm{GeV}$ and $\left|\eta^{\mathrm{jet}}\right| < 1.6$ in collisions at $\sqrt{s} = 13\,\mathrm{TeV}$, comparing data with PYTHIA8 predictions.

Building on previous two-particle correlation studies, where the trigger and associated particles were selected from the same j_{T} range, this analysis investigates cases with differing $j_{\mathrm{T}}^{\mathrm{trg}}$ and $j_{\mathrm{T}}^{\mathrm{ass}}$. This extension provides deeper insights into the origins of two-particle correlations across different momentum scales. The second-order Fourier coefficient of the two-particle correlation function is presented in Figs. 2, as a function of $j_{\mathrm{T}}^{\mathrm{trg}}$ for various $N_{\mathrm{ch}}^{\mathrm{j}}$ bins, with associated particles in the range $0.3 < j_{\mathrm{T}}^{\mathrm{ass}} < 3\,\mathrm{GeV}$. The PYTHIA8 predictions generally agree with the data for most $N_{\mathrm{ch}}^{\mathrm{j}}$ intervals. However, for the highest $N_{\mathrm{ch}}^{\mathrm{j}}$ bin, an enhancement of $V^*_{2\Delta}$ relative to MC predictions is seen for $0.5 < j_{\mathrm{T}}^{\mathrm{trg}} < 1\,\mathrm{GeV}$. This observation is qualitatively consistent with correlations where $j_{\mathrm{T}}^{\mathrm{trg}}$ and $j_{\mathrm{T}}^{\mathrm{ass}}$ lie in the same range.

3.2 Jet substructure engineering

To probe the connection between long-range anisotropy and initial-state geometry, jets are classified by substructure using the $z_g\theta_g$ observable. Large values of $z_g\theta_g$ select jets with a clear two-prong topology, characterized by both a more balanced p_{T} sharing and a wider angular separation between sub-jets, features that may correspond to a larger initial-state eccentricity during the early stage of parton shower. Figure 3 shows v_2^* versus $N_{\mathrm{ch}}^{\mathrm{j}}$ for jets separated into $z_g\theta_g < 0.25$ and $z_g\theta_g > 0.25$, compared to PYTHIA8. larger values of $z_g\theta_g$ generally exhibit a higher v_2^*, likely due to the azimuthal back-to-back configuration of their sub-jets. This is consistent with dijet fragmentation but could also reflect sensitivity to collective flow. For large $z_g\theta_g$, v_2^* increases with $N_{\mathrm{ch}}^{\mathrm{j}}$for $N_{\mathrm{ch}}^{\mathrm{j}} > 80$, while for smaller $z_g\theta_g$, it tends to decrease at high $N_{\mathrm{ch}}^{\mathrm{j}}$, suggesting a link between jet shape and long-range correlations. Notably, PYTHIA8 predicts a decreasing v_2^* with $N_{\mathrm{ch}}^{\mathrm{j}}$for both small and large $z_g\theta_g$, contrasting the data. The observed structure-dependent enhancement of v_2^* implies a possible influence of intrinsic partonic interactions and associated dynamics.

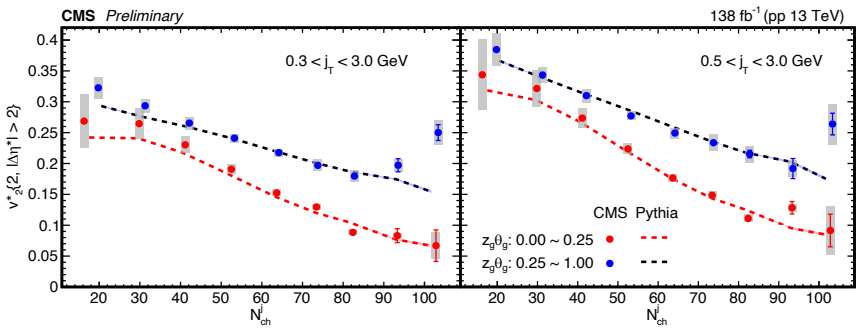

Figure 3. The elliptic anisotropy v_2^*, obtained from two-particle correlations, as a function of $N_{\mathrm{ch}}^{\mathrm{j}}$ for two jet substructure classes, $z_g\theta_g < 0.25$ (red) and $z_g\theta_g > 0.25$ (blue). Results are presented for two transverse momentum ranges, $0.3 < j_{\mathrm{T}} < 3\,\mathrm{GeV}$ (left) and $0.5 < j_{\mathrm{T}} < 3\,\mathrm{GeV}$ (right), using anti- jets with R = 0.8, $p_{\mathrm{T}}^{\mathrm{jet}} > 550\,\mathrm{GeV}$, and $\left|\eta^{\mathrm{jet}}\right| < 1.6$ in collisions at $\sqrt{s} = 13\,\mathrm{TeV}$. The data points include statistical uncertainties (vertical bars), while systematic uncertainties are indicated by shaded boxes. The shaded envelopes around the PYTHIA8 curves represent statistical uncertainties.

4 Summary

The phenomenon of long-range azimuthal anisotropy in high-multiplicity jets is systematically investigated, and the origin of long-range correlations is explored by jet substructure engineering. An enhancement of v_2^* at high $N_{\mathrm{ch}}^{\mathrm{j}}$ is observed only in two-prong jets, indicating a possible connection to the initial jet geometry. Further model studies are required to establish the underlying dynamics.

References

[1] K. Dusling, W. Li, B. Schenke, Novel collective phenomena in high-energy proton-proton and proton-nucleus collisions, Int. J. Mod. Phys. E **25**, 1630002 (2016), 1509.07939. 10.1142/S0218301316300022

[2] A. Baty, P. Gardner, W. Li, Novel observables for exploring QCD collective evolution and quantum entanglement within individual jets, Phys. Rev. C **107**, 064908 (2023), 2104.11735. 10.1103/PhysRevC.107.064908

[3] A. Hayrapetyan et al. (CMS), Observation of enhanced long-range elliptic anisotropies inside high-multiplicity jets in pp collisions at $\sqrt{s} = 13\,\mathrm{TeV}$, Phys. Rev. Lett. **133**, 142301 (2024), 2312.17103. 10.1103/PhysRevLett.133.142301

[4] W. Zhao, Z.W. Lin, X.N. Wang (2024), 2401.13137

[5] M. Cacciari, G.P. Salam, G. Soyez, FastJet user manual, Eur. Phys. J. C **72**, 1896 (2012), 1111.6097. 10.1140/epjc/s10052-012-1896-2

[6] S. Chatrchyan et al. (CMS), Description and performance of track and primary-vertex reconstruction with the CMS tracker, JINST **9**, P10009 (2014), 1405.6569. 10.1088/1748-0221/9/10/P10009

[7] A.M. Sirunyan et al. (CMS), Pileup mitigation at CMS in 13 TeV data, JINST **15**, P09018 (2020), 2003.00503. 10.1088/1748-0221/15/09/p09018

[8] D. Bertolini, P. Harris, M. Low, N. Tran, Pileup per particle identification, JHEP **10**, 059 (2014), 1407.6013. 10.1007/JHEP10(2014)059